THE CHARACTERISTICS AND APPLICATIONS OF CERAMIC LASER FUSION AND CERAMIC LASER SINTERING

H. H. Tang[1], H. C. Yen[1,*], M. L. Chiu[2], J. H. Jou[3]

[1] Department of Mechanical Engineering, National Taipei University of Technology

[2] Graduate Institute of Mechanical and Electrical Technology, National Taipei University of Technology

[3] Graduate Institute of Manufacturing Technology, National Taipei University of Technology

*Corresponding author Reviewed, accepted September 10, 2008

Abstract

The aim of present study is to investigate the possible application of the ceramic parts which are fabricated with the process of Ceramic Laser Fusion or Ceramic Laser Sintering. The experimental results reveal: (1) CLF can lead to a reduction in the porosity of the ceramic part but also can induce micro-cracks. Therefore, this process cannot produce a part with the required strength by a post-process of infiltration; (2) CLS is capable of fabricating a ceramic part with high porosity. By adjusting the slurry formulation and varying the scanning energy, the open porosity can be over 90vol% of the total porosity. After a post-process of infiltration, the density can be increased to 95%; therefore, CLS can apply to produce a part with high strength. Because the high open porosity leads to a good permeability, the process of CLS is suitable for the fabrication of ceramic shell mold.

Keywords: Ceramic Laser Fusion; Ceramic Laser Sintering; porosity; ceramic shell mold

1. Introduction

Rapid Prototyping is a non-traditional technology based on layer manufacturing. To date, some processes have been commercialized, such as Stereolithography (SL)[1,2], Selective Laser Sintering (SLS)[3,4], Laminated Object Manufacturing (LOM)[5,6], and 3D Printing (3DP)[7,8]; all these techniques have the potential of fabricating ceramic parts. Owing to the demand of producing ceramic functional parts, some researches are switched to investigating the feasibility of fabricating ceramic components based on those processes.

Tang[9,10] invented two rapid prototyping processes, Ceramic Laser Fusion (CLF) and Ceramic Laser Sintering (CLS), in 2001 and 2007 respectively. Both processes are somewhat similar to SLS in principle of using laser scanning to fabricate parts; nevertheless, instead of using loose powder in SLS, slurry which consists of ceramic powder and inorganic binders is employed in CLF/CLS. The ceramic slurry allows the use of smaller ceramic particles to cast ultra-thin layer which leads to a higher green density. Both processes have identical manufacturing steps but different working temperature. During the laser scanning, the working temperature of CLF is higher than the melting point of the ‘high melting point’

ceramic powder; because the high melting point ceramic powder is melted, the consolidation mechanism is defined as 'fusion' in this paper. On the other hand, the working temperature of CLS is lower than the melting point of the high melting point ceramic powder, but higher than the melting point of the low melting point ceramic powder; consequently, the high melting point ceramic powder remains solid while the molten low melting point ceramic powder spreads between the solid particles almost instantaneously as it is driven by intense capillary forces; the binding mechanism is defined as 'sintering' in this paper. The 'high melting point' ceramic powder is so-called the structural material, while the 'low melting point' material is then what is called the binder.

The part density is correlated with the working temperature. Actually, CLF and CLS have a different working temperature to each other. By comparison with CLS, the parts fabricated by CLF can achieve a higher density and strength without any post-process of densification. The parts fabricated by these two processes demonstrate different structure characteristics to one another. The aim of current study is to investigate characteristics and applications of the parts made by these two processes. The slurry based rapid prototyping technology with controlled laser energy was utilized to fabricate ceramic parts for measuring the part porosity and evaluating the part's mechanical characteristics. Eventually, the feasibility of both processes for producing the parts with high or low mechanical strength was evaluated.

2. Experimental procedure

Technology for fabricating ceramic parts by CLF is well established. The slurry formulation, consolidation mechanism, and laser scanning parameters for CLS were investigated by Yen[11]; a knowledge base was built to establish the relationship among the scanning line width, scanning line depth, consolidation mechanism, and working parameters; it is in favor of selecting parameters for experiments.

To fabricate a 3D part, fabricating a specimen (Fig. 1) to obtain scanning line width and depth in advance is a must. A layer with a thickness of 10 μm for observing the scanning depth was fabricated on a pre-fabricated solid base. Afterward, some spacers were built on the top of observing layer, and another layer with several separated scanning lines for observing the scanning line width was fabricated on the top of spacers. After the process of green part removal, the depth of overhang, which is the scanning line depth, and the scanning line width were measured by an optical microscope equipped with an X-Y platform driven by micrometer head. Based on the collected data, the scanning space and the layer thickness for fabricating a full melting part can be achieved. A CO_2 laser has been used in this experiment. Scanning energy density is varied with laser beam size, laser power and scanning speed;

selecting a suitable parameter combination to achieve a high energy density laser scanning is the principle of building a fusion specimen. After the green part removal, the consolidation mechanism can be verified by observing the topography with a Scanning Electron Microscope (SEM).

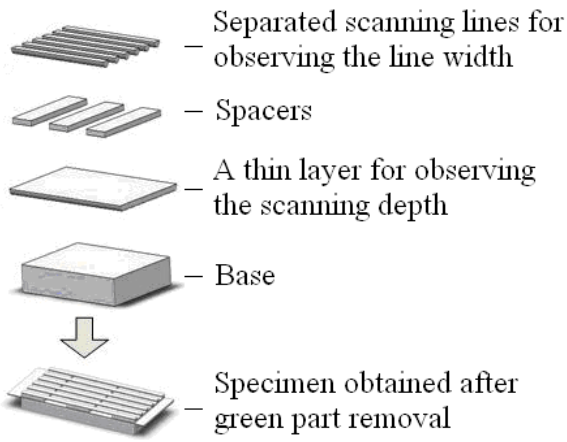

Fig. 1 Schematic of fabricating a specimen for measuring scanning line width and depth

2.1 Fused specimens fabricated by Ceramic Laser Fusion

In the present study, the material was prepared with the proportion of 52.63 wt% silica, 3.68 wt% clay, 1.58 wt% silica sol, and 42.11 wt% water. Particle size of silica is 11~15 μm. The well-dispersed slurry was obtained by mixing the slurry with an electric blender for 12 hours. A 10 x 10 mm fused specimen was made by scanning a laser beam over the surface of the green layer. The layer thickness was 40 μm. The laser was operated at laser power of 19W with a scan speed of 60 mm/s and scanning space of 0.1 mm; this scanning parameter combination led to a linear overlap of 80%, and a planar overlap of 80%.

2.2 Sintered specimens fabricated by Ceramic Laser Sintering

Two different compositions of the slurry were used as shown in Table 1. Slurry I contained more binders than slurry II did. Layer with a thickness of 20 μm was casted on a working platform which was preheated to 90 ℃. Following the same process as mentioned in section 2.1, the specimens were fabricated for measuring the scanning line width and depth. By collaborating with a variety of laser power, a 10 x 10 mm sintered specimens was fabricated with a parameter combination as following: scanning speed of 500 mm/s, laser power of 14W, scanning spacing of 0.15 mm, layer thickness of 20 μm, linear overlap of 75%, planar overlap of 55%; and de-focus of 4.75 mm.

Table 1 The composition of the slurry for fabricating ceramic sintering specimens

	SiO_2 (g)	Clay (g)	Silica sol (g)
Slurry I	100	7	9
Slurry II	100	3	7

2.3 Porosity measurement

The liquefied wax was infiltrated into the open pores between the solid by capillary forces. Equations 1~6 can be used to individually figure out bulk density, open porosity and closed porosity of the part. "A" represents the weight of a laser sintered part which was measured after cooling at room temperature for an hour. The specimen was immersed in the 70 ℃ liquefied wax for 30 minutes, and then taken out for cooling at room temperature for 30 minutes. "B" represents the weight of the infiltrated specimen. "C" represents the weight of the infiltrated specimen which was weighted during it was immersed in a tank filled up with 25 ℃ water. The theoretical density of SiO_2 and wax are 2.7 g/cm^3 and 0.9 g/cm^3 respectively.

$$V_{all} = \frac{B - C}{D_{water}} \quad (1)$$

$$V_o = \frac{B - A}{D_{wax}} \quad (2)$$

$$V_c = V_{all} - V_o - \frac{A}{D_{silica}} \quad (3)$$

$$Bulk\ Density = \frac{A}{V_{all} - V_o} \quad (4)$$

$$Open\ Porosity(\%) = \frac{V_o}{V_{all}} \times 100 \quad (5)$$

$$Closed\ Porosity(\%) = \frac{V_c}{V_{all}} \times 100 \quad (6)$$

V_{all} : total volume of the part; V_o : total volume of the open pores; V_c: total volume of the closed pores; D: density

3. Results and discussion

Thermal energy delivered from a laser is absorbed by the green part, and is transferred from the surface to the interior. Fig. 2 schematically shows a temperature distribution corresponding to the energy distribution of the Gaussian beam which has the maximum energy intensity at the beam midpoint. Under the condition of constant scanning speed and beam size, as the laser power is raised to a certain value, the scanned surface will reach the melting point of the clay (~1200℃), the melted clay binds the solid silica particles to produce

a liquid phase sintering zone. If the laser power is continuously increased, the silica particles on the surface will be melted, and the fusion zone will extend from the surface to the interior of the green part. The area below the fusion zone is the sintering zone as mentioned above. The property transformation zone, which includes the fusion zone and sintering zone, can be taken apart from the green block by a green part removal operation. D_{pt} and W_L represent the scanning line depth and width respectively. If the layer thickness is smaller than the fusion zone depth, the fusion zone of each layer will be overlapped; then the fusion part can be manufactured.

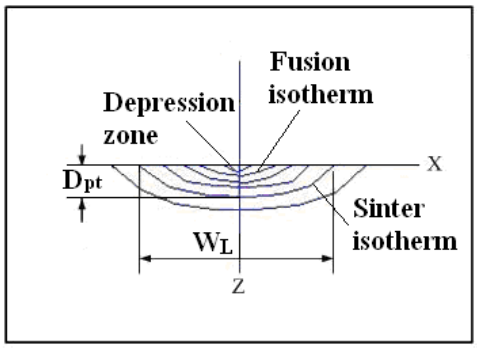

Fig. 2 Temperature distribution corresponding to the energy distribution of the Gaussian beam

3.1 The characteristics of the fusion part

The topography shown in Fig. 3 is the surface of the fusion part fabricated with the parameter combination mentioned in sec. 2.1. The surface is not smooth and has many depressions. A few closed pores are also included in the interior of the fusion part; however, the porosity is lower than that of the sintering part. Moreover, cracks are brought out along the direction perpendicular to the scanning line. The full fusion parts made with other scanning parameters have the same results. Consequently, high density, rough surface, and closed pores are the characteristics of the fusion ceramic part.

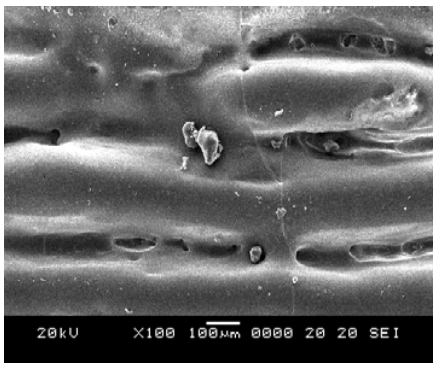

Fig. 3 The topography of the fusion part

The fusion part provides a higher density than the sintering part does and can result a higher mechanical strength; however, the high density is resulted from the full melting ceramic powder, but the fusion part contains a large number of micro-cracks which is evenly distributed throughout the part and deteriorates the strength of the fusion part. As the ceramic is a brittle material, its tensile strength is only one tenth of its compressive strength and it can hardly deform plastically; therefore, thermal stress will easily induce micro-cracks. In current investigation, in order to achieve full melting, a high laser power with a low scanning speed was employed. Due to the continuous scanning, the surface temperature increases rapidly; therefore, the thermal expansion on the surface is larger than that at the interior of the part. The surface and the interior of the part bear compressive stress and tensile stress respectively; after scanning, the scanned surface contacts the cold air in the atmosphere; therefore, the cooling speed on the surface is faster than that in the interior while the stress direction is opposite to the trend of temperature rising; such phenomenon easily leads to crack formation during the manufacturing process.

3.2 The characteristics of the sintering part

Some specimens for measuring the scanning line width and depth were fabricated with the parameter combination and slurry I shown in section 2.2. As a result, the average scanning line width was 0.49 mm and depth was 0.045 mm. Based on these data, a part can be fabricated with sintering consolidation mechanism. Fig. 4 shows some 10×10×1 (mm） ceramic sintering parts. Fig. 5(a) and 5(c) demonstrate their surface and cross-section. Fig. 5(a) shows that sintering consolidation appears on the surface. Although a partial melting occurs locally, the individual molten area is less than 20×20 μm and does not connect with each other. Fig. 5(c) reveals the sintering part is porous and no extensive melting area, which prohibits the connection of the pores, exists between the layers.

The surface of the part shows more melting state when the laser power was increased to 16W. Fig. 5(b) and 5(d) demonstrate their surface and cross-section. The melted silica fills up the pores on the surface. An extreme thin fusion layer exists between the two layers as shown in Fig. 5(d); such fusion layer obstructs the interconnection of the pores on the boundary of the layers, and then reduces the amount of open pores dramatically. By collaborating with a variety of laser power, de-focus distance of 4.75 mm, and scanning speed of 500 mm/s, the porous sintering parts also can be fabricated with the slurry II which contains less binder as mentioned in section 2.2.

Fig. 4 Parts (10 x 10 mm) fabricated by the process of Ceramic Laser sintering

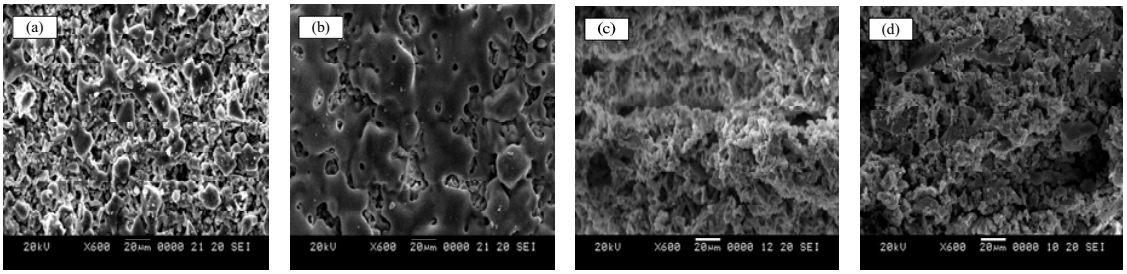

Fig. 5 (a) The topography of the part built with a laser power of 14 Watts
(b) The topography of the part built with a laser power of 16 Watts
(c) The cross section of the part built with a laser power of 14 Watts
(d) The cross section of the part built with a laser power of 16 Watts

3.3 The porosity of the ceramic sintering parts

Table 2 shows the porosity of the parts fabricated with different laser power and two kinds of slurry mentioned in section 2.2. The total porosity of the sintering part made of slurry I is 46%, but the closed porosity is higher than that in the part made of slurry II. If a low melting point material infiltrates into such parts, the highest density is only 84%. This can be explained that the molten clay blocks up a part of pores to form closed pores during the process of binder melting so that the number of the closed pores is increased. Owing to the higher proportion of the binder, the closed porosity of the part fabricated with the slurry I is higher than that of the part fabricated with the slurry II.

Table 2 The porosity of the parts fabricated with different laser powers and two kinds of slurry listed in Table 1

	Laser Power (W)	Open porosity (%)	Closed porosity (%)
Slurry I	14	30	16
Slurry II	10	38	7.8
	8	37	7.4
	10 (with post-sintering)	40.6	5.2
	8 (with post-sintering)	42.5	4.1

For the slurry II, a minor adjustment of the laser power can not lead to an obvious variation of the total porosity. The total porosity of the slurry II is almost the same as the result of the slurry I; however, because the proportion of the binder is only 10vol% of the total ceramic materials, the closed porosity of the slurry II is reduced to 7~8％ while the open porosity is increased to38%. When a low melting point material infiltrates into the sintering part, the density is increased to 92%. Furthermore, when the sintering part is put into a furnace with a constant temperature 1150 ℃ for 2 hours, the total porosity is almost not changed, but the closed porosity is reduced around 3％ while the open porosity is increased to 40 ~ 42% and the density can be increased to 95% if it is infiltrated afterwards. Fig. 6(a) is the cross section of the part which is fabricated with a laser power of 8W with a thermal post-sintering; Fig. 6(b) is the cross section of the part infiltrated with wax.

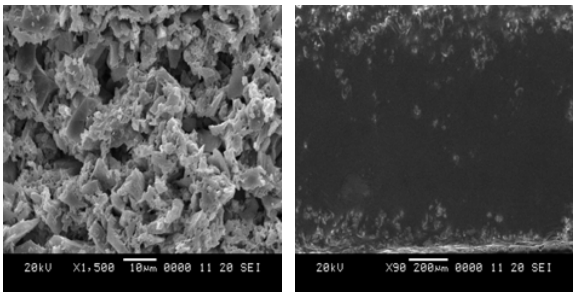

Fig. 6 (a) The cross section of the part which was fabricated with a laser power 8W and a process of post-sintering; (b) the cross section of the part infiltrated with wax

4. Conclusion

According to the characteristics of the fusion part and the sintering part mentioned above, we can evaluate the feasibility of applying these two methods for producing parts with high mechanical strength and parts with low mechanical strength.

In comparison with CLS, CLF can lead to a reduction in porosity and a higher density. Because silica is a brittle material, a high energy laser scanning easily leads to thermal crack on the part; such cracking might bring a minor defective to a destructive crack development. Because a great portion of the pores in the fused structure are closed, the molten material can not be infiltrated into the pores of the fused structure; therefore, the mechanical strength of the part can not be increased by infiltration. Obviously, CLF is also not suitable for the part which needs high permeability, such as ceramic shell mold for precision casting.

CLS can be used to fabricate the part with high porosity. By changing the slurry formulation and varying the scanning energy, the open porosity can be adjusted. The results of the experiments demonstrate that the total porosity of a sintering part can be greater than

45% and the open porosity can be greater than 90% of the total porosity. After infiltrating, the density of the part can increase to 95%; such process can be employed for the part needs high mechanical strength. Besides, the high open porosity leads to the process of CLS is also suitable for manufacturing ceramic shell mold which needs high permeability.

The future work will concentrate on CLS to fabricate ceramic part with high open porosity for the products need high permeability, such as ceramic filter and ceramic shell mold. For the part needing high mechanical strength, a post-process of infiltrating a high strength metal or non-metal material could follow the process of CLS.

Acknowledgement

This work was supported by National Science Council of ROC under project NSC96-2221-E-027-103-MY2.

Reference

1. J. W. Halloran, M. Griffith, and T. Chu, "Stereo-Lithography Resin for Rapid Prototyping of Ceramics and Metals", U.S. Patent Application 6,117,612, 2000
2. M. L. Griffith and J. W. Halloran, "Freeform Fabrication of Ceramics via Stereolithography", Journal of the American Ceramic Society, Vol. **79**, no. 10, 1996, pp 2601 - 2608
3. F. Klocke and H. Wirtz, "Selective Laser Sintering of Zirconium Silicate", Proc. of The 9th Solid Freeform Fabrication Symposium, The University of Texas at Austin, Texas, USA, 1998, pp 605 - 612
4. P. K. Subramanian, N. Vail, J. W. Barlow and H. L. Marcus, "Selective Laser Sintering of Alumna with Polymer Binders", Rapid Prototyping Journal, Vol. **1**, 1995, pp 24 – 35
5. D. Klosterman, "Laminated Object Manufacturing (LOM) of Advanced Ceramic and Composites", Proc. of the 7th International Conference on RP, University of Dayton and Stanford U., San Francisco, CA, USA, 1997, pp 43 - 50
6. C. Griffin, J. Daufenbach and S. McMillin, "Solid Freeform Fabrication of Functional Ceramic Components Using a Laminated Object Manufacturing Technique", Proc. of the 5th Solid Freeform Fabrication Symposium, The University of Texas at Austin, Texas, USA, 1994, pp 17 - 24
7. E. M. Sachs, A. Curodeau, T. Fan, J. F. Bredt, M. J. Cima and D. Brancazio, "Three Dimensional Printing System", United States Patent 5,807,437, 1998
8. J. Grau, J. Moon, S. Uhland, M. Cima and E. Sachs, "High Green Density Ceramic Components Fabricated by the Slurry-based 3DP Process", Proc. of the 8th Solid Freeform Fabrication Symposium, The University of Texas at Austin, Texas, USA, 1997, pp 371 - 378

9. H. H. Tang, “Method for rapid forming of a ceramic work piece”, U.S. patent no. 6217816, 2001
10. H. H. Tang, “Building Ultra-Thin Layers by Ceramic Laser Sintering”, Materials Transactions, Journal of The Japan Institute of Metals, Vol. **47**(3), 2006, pp 889 - 897
11. H. C. Yen, “The Research and Development of Ceramic Laser Sintering in Rapid Prototyping Technology”, Ph.D. Thesis, National Taipei University of Technology, Taipei, 2007